Metabolic Engineering 60 (2020) 66–76

Contents lists available at ScienceDirect

Metabolic Engineering

journal homepage: www.elsevier.com/locate/meteng

Original Research Article

Combining genetically-encoded biosensors with high throughput strain screening to maximize erythritol production in *Yarrowia lipolytica*

Xueliang Qiu[a], Peng Xu[e], Xinrui Zhao[a,d], Guocheng Du[a,c], Juan Zhang[b,c,*], Jianghua Li[a,d,**]

[a] School of Biotechnology, Jiangnan University, 1800 Lihu Road, Wuxi, 214122, Jiangsu, China
[b] Key Laboratory of Industrial Biotechnology, Ministry of Education, School of Biotechnology, Jiangnan University, 1800 Lihu Road, Wuxi, 214122, Jiangsu, China
[c] The Key Laboratory of Carbohydrate Chemistry and Biotechnology, Ministry of Education, Jiangnan University, 1800 Lihu Road, Wuxi, 214122, Jiangsu, China
[d] National Engineering Laboratory for Cereal Fermentation Technology, Jiangnan University, 1800 Lihu Road, Wuxi, 214122, Jiangsu, China
[e] Department of Chemical, Biochemical and Environmental Engineering, University of Maryland Baltimore County, Baltimore, MD, 21250, USA

ARTICLE INFO

Keywords:
EryD
Biosensor
High throughput screening
Erythritol
Yarrowia lipolytica

ABSTRACT

Erythritol is an important sweetener ingredient and chemical precursor for synthesizing materials with phase transition behavior. Commercial erythritol is primarily produced by industrial fermentation. Further strain engineering necessitates the development of high throughput screening method for rapid detection and screening of mutant strain libraries. In this work, we took advantage of the erythritol-responsive transcription factor EryD, and constructed a sensor-regulator system for rapid screening and characterization of erythritol overproducers. We configured the optimal architecture of the EryD sensor-regulator construct with improved sensitivity, specificity and dynamic response range. Coupled with mutagenesis and strain screening based on biosensors, we rapidly screened and characterized a strain library containing 1152 mutants derived from combined UV and ARTP mutagenesis, in a relatively short period of time (1 week). The optimal strain produced more than 148 g/L erythritol in bench-top reactors. This work provides a reference for other metabolic engineering researchers to develop industrially-relevant strains. The reported framework enables us to rapidly improve strain performance and engineer efficient microbial cell factories for industrial applications.

1. Introduction

Erythritol has been widely used as a low-calorie sweetener in foods and beverage industry. Physiochemical characterization indicates its important phase transition behavior during material synthesis (Raymundo et al., 2018). In addition, erythritol may serve as precursor for the production of 1,4-butanediol, 3-butene-1,2-diol and other important functional materials (Dai et al., 2019; Tshibalonza et al., 2018). Nowadays, commercial erythritol is primarily produced by fermentation with *Yarrowia lipolytica* from glucose (Silva et al., 2018). However, due to the lacking of high throughput screening method for erythritol, obtaining high-producing strains is always a challenging task for strain development and characterization. The highest titer obtained by metabolic engineering in *Yarrowia lipolytica* reported to date is about 80.6 g/L in bench-top reactors (Carly et al., 2017).

To improve the cost-efficiency, mutagenesis and metabolic engineering are the key components to improve the yield, productivity and titers of erythritol production (Carly and Fickers, 2018). The quantification of erythritol mainly depends on HPLC or chemical coloration (Zhang et al., 2015). However, the long retention time of HPLC and the nontrivial derivatization of chemical coloration is time-consuming and laborious, which significantly limits strain development when a large library of mutant was obtained. Periodate oxidation and thin-layer chromatography (TLC) have been developed for the rapid detection of erythritol (Wang et al., 2013). Due to complex procedures and the interference of fermentation substrates, the detection results vary significantly with big noise, which make this method difficult to be used in practical work. Therefore, there is a pressing need to develop high throughput screening methods to accelerate the strain development process.

Ery Operon is a functional gene cluster consisting of erythritol metabolic genes, which is known to be induced by erythritol in *Brucella* species (Sangari et al., 2000). The lacks of phosphoenolpyruvate synthase and phosphofructokinase genes in all *brucellae* confirm previous evidence that glycolysis is missing (Barbier et al., 2018). Because the inefficiency of the Entner–Doudoroff pathway to provide energy for the

* Corresponding author. School of Biotechnology, Jiangnan University, 1800 Lihu Road, Wuxi, 214122, Jiangsu, China.
** Corresponding author. School of Biotechnology, Jiangnan University, 1800 Lihu Road, Wuxi, 214122, Jiangsu, China.
E-mail addresses: zhangj@jiangnan.edu.cn (J. Zhang), lijianghua@jiangnan.edu.cn (J. Li).

https://doi.org/10.1016/j.ymben.2020.03.006
Received 2 November 2019; Received in revised form 13 March 2020; Accepted 15 March 2020
Available online 26 March 2020

Abbreviations

HTS	High throughput screening
SMB	Synthetic microbial biosensor
HPLC	High performance liquid chromatography
DBD	DNA binding domain
UV	Ultraviolet
ARTP	Atmospheric room temperature plasma
AMP-IPTG	Ampicillin and isopropyl β-D-thiogalactoside
RFI	Relative fluorescence intensity
FI	Fluorescence intensity
DO	Dissolved oxygen
SLM	Standard liter per minute
HG	Fermentation medium with high glucose
DBS	DNA binding sequence
eGFP	Enhanced green fluorescent protein
TLC	Thin-layer chromatography
RBS	Ribosome binding sites
ITC	Isothermal titration calorimetry
LB	Luria-Bertani
TTC	2,3,5-triphenyl tetrazolium chlorid
OD_{600}	Optical density at 600 nm
UAS	Upstream activation sequences

proliferation of *Brucella*, *Brucella* species have evolved to metabolize erythritol and takes advantage of pentose phosphate pathway to produce energy and carbon backbones for cell growth and metabolic synthesis. Therefore, Ery Operon played an important role to bridge the gap between erythritol degradation and energy production by pentose phosphate pathway. This operon is composed of three functional genes EryA, EryB and EryC, encoding the erythritol-degradation pathways, and a transcription repressor EryD whose DNA-binding affinity is dependent on the level of erythritol in the cell (Zhang et al., 2014). The three genes EryA, EryB and EryC encode a putative erythritol kinase, an erythritol phosphate dehydrogenase and a D-erythrulose-1-phosphate dehydrogenase, respectively. EryD is a transcriptional factor repressing the expression of EryABC in the absence of erythritol. But when erythritol appears, erythritol binds with EryD and induce a conformational change so EryD dissociates from the Ery Operon and allow the EryABC to be transcribed (Fig. 1). The highly specific response of EryD to erythritol, presumably, provides us an ideal molecular switch for the development of high throughput screening tools for erythritol-producing strains. Inspired by the one-pot two-strain system (Zheng et al., 2018), we explored the utility of EryD to develop a high throughput screening method for rapid detection of erythritol and characterization of strain performance.

In this work, the hybrid T7 system consisting of EryD transcriptional repressor and putative operator sequence of Ery Operon was optimized to control T7 promoter activity in *E. coli* BL21(DE3) and the whole cell was named as synthetic microbial biosensor (SMB) system. With fluorescence reporter, we configured the optimal architecture of the EryD sensor system construct with improved sensitivity, specificity and dynamic response range. Coupled with mutagenesis and automatic strain screening, we were able to screen and characterize more than 1152 strains in a relatively short period of time (1 week) (Fig. 2). This is the first report to develop EryD as high throughput biosensor to improve strain performance. The chosen strain produced more than 148 g/L erythritol in bench-top reactors. This work expands our ability to improve strain performance and provides a reference for other microbial metabolic engineering researchers to develop industrially relevant strains for various applications.

2. Materials and methods

2.1. Strains, plasmids, and medium

The strains, plasmids and primers used in this study are listed in Table 1. *E. coli* was cultivated in Luria-Bertani (LB) medium (Jira et al., 2018). *Yarrowia lipolytica* seed culture was prepared in yeast extract peptone dextrose (YPD) medium (Albers and Larsson, 2009). High throughput screening of strains were carried out in HG medium. The compositions of the mediums are as follows, LB: Tryptone 10 g/L, Nacl 10 g/L, Yeast Extract 5 g/L; YPD: Glucose 20 g/L, Yeast Extract 10 g/L, Tryptone 20 g/L; HG: Glucose 150 g/L, Yeast Extract 10 g/L, Ammonium Citrate 5 g/L, Magnesium Sulphate 0.5 g/L, Potassium Dihydrogen Phosphate 0.25 g/L. In all the solid mediums, 20 g/L agarose was added.

2.2. Purification of EryD and determination of binding affinity with Isothermal Titration Calorimetry

EryD was expressed in *E. coli* BL21(DE3) and cultured in LB medium. When the optical density at 600 nm (OD_{600}) of culture reached about 1, 0.5 mM IPTG was added and induced at 16 °C for 9 h. Then, cells were collected by centrifugation at 5000 rpm. Subsequently, one tenth volume of deionized water was added to suspend the cell pellet. High-pressure homogenizer (UH-06, Union-biotech, China) was used to break up the cells. The crushing pressure was 1000 bar, and the

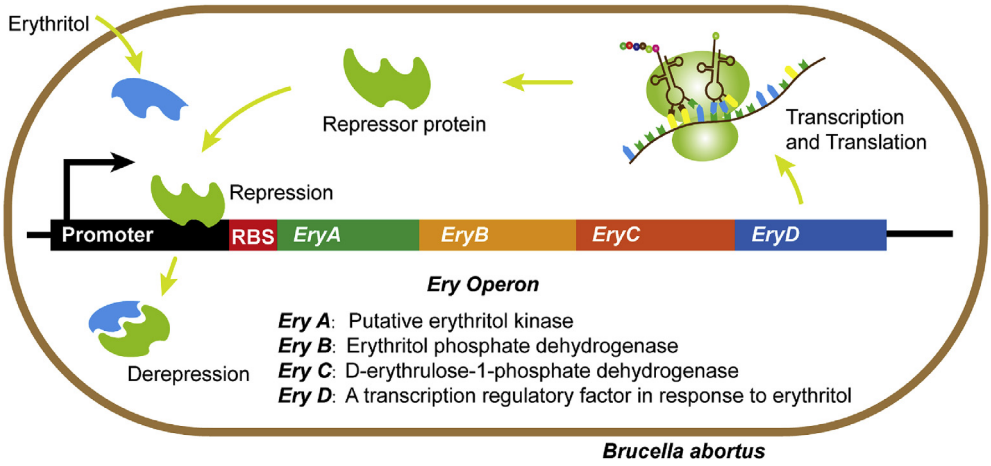

Fig. 1. The structure and visualization of Ery Operon in *Brucella abortus*.

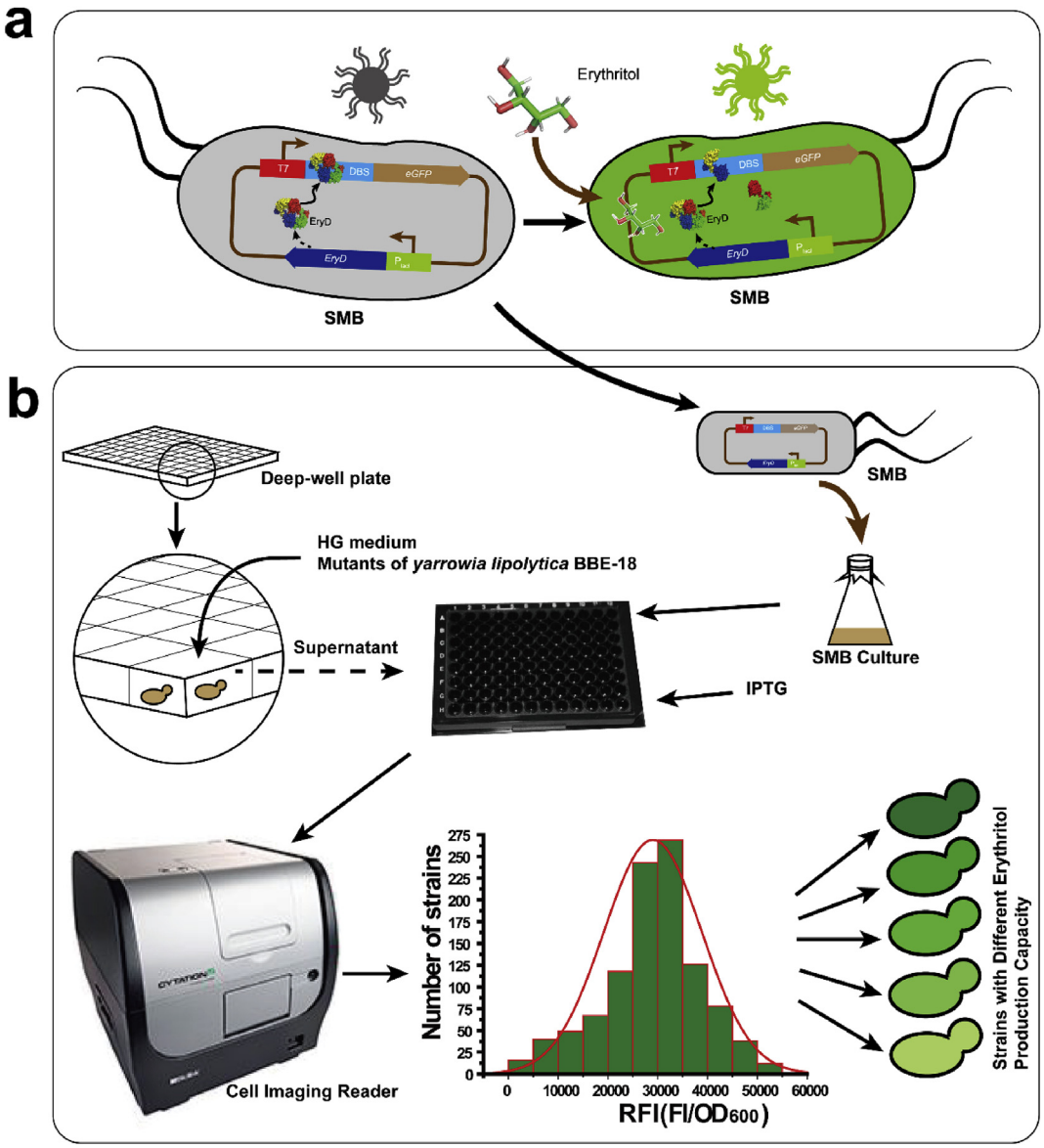

Fig. 2. The working flowchart of SMB system based on EryD and its application for high throughput screening (HTS) of erythritol-producing strains. a. In the absence of erythritol, EryD expressed in SMB system binds to the promoter region and represses the expression of eGFP. In the presence of erythritol, EryD tetramer is decomposed to two dimers. Then the RNA polymerase can proceed with transcription, so that the eGFP gene can express normally to output fluorescence signals. b. Rapid sorting of erythritol-producing strains by SMB system. *Yarrowia lipolytica* BBE-18 mutants were fermented in HG medium in deep-well plates and the supernatant was transferred to 96-well plates with peripheral opacity. Then the cultured SMB cells were added and the fluorescence detection was carried out after the appropriate time of cultivation. According to the relative fluorescence intensity (RFI), the abilities of erythritol-producing strains were sorted.

sample volume was 100 ml per batch. After two times of crushing, the liquid was transparent, and the cell debris was removed by centrifugation at 12000 rpm. With protein purification instrument (AKTA™, GE Healthcare Bio-Sciences, Sweden), the transparent cell breakup solution was purified with nickel column, impurities were eluted with 15% imidazole solution, and EryD was eluted with 45% imidazole solution. The interactions between EryD, DNA-binding sites and erythritol were measured by Isothermal Titration Calorimetry (ITC) (NANO ITC. TA Instruments, Germany), following the company's protocol.

2.3. Construction of synthetic microbial biosensor system

Gibson Assembly (Gibson et al., 2009, 2010) was used to construct plasmids. EryD gene was synthesized by Genscript Company and expressed with plasmid PUC57 in *E. coli* JM109. The SMB reported in this paper was constructed with the skeleton of pET-22b(+) (Mahmood et al., 2019). The gene sequence of EryD and its possible DNA binding sequence (DBS) were used to replace *lacO* and *lacI* in pET-22b(+), respectively. *E. coli* BL21(DE3) was used as the host for the SMB and *E. coli* JM109 was used for the storage of plasmids. Competent cells of *E. coli* JM109 (Bolognese et al., 2019) and *E. coli* BL21(DE3) were prepared with High-efficiency Competent Cell Preps Kit (B529305-0200, Sangon Biotech, Shanghai, China). Plasmids were extracted by SanPrep Column Plasmid Mini-Preps Kit (B518191-0100, Sangon Biotech, Shanghai, China).

For transformation, 100 μl competent cells of *E. coli* BL21(DE3) were loaded into a 1.5 ml centrifuge tube, immediately mixed with 10 μl plasmid and incubated on ice for 40 min. After hot incubation for 90 s at 42 °C, the mixture was placed on ice for 3 min. Under sterile conditions, 1 ml LB medium was added into the tube and incubated at 37 °C for 1 h. Most of the supernatant was removed after centrifugated

Table 1
Strains, plasmids and methods.

Strain or plasmid	Characteristics	Source
Strains		
E. coli BL21(DE3)		Sangon Biotech. China
E. coli JM109		Sangon Biotech. China
Yarrowia lipolytica BBE-18		CCTCC M 2019163
Plasmids		
pEryD		GenScript Biotech Corp.
pDBS		GenScript Biotech Corp.
pGFP	Based on pET-22b(+)-EryD.	
pEDG	pET-22b(+) carrying the genes of EryD, GFP and the possible DNA binding sequences of EryD-expressed proteins named DBS.	This work.
pKEDG	Based on pET-22b(+)-EryD-DBS-GFP.	This work.
pKEDG-K16	Based on pET-22b(+)-KEryD-DBS-GFP	This work.
pKEDG-inRBS	Based on pET-22b(+)-KEryD-DBS-GFP	This work.
pGLDLE	Based on pET-22b(+)-EryD and pUC57-DBS.	This work.
pGLDU96-LE	Based on pET-22b(+)-GFP-LacO::DBS(1–200)-LacI::EryD	This work.
pGKDLE	Based on pET-22b(+)-GFP-LacO::DBS(1–200)-LacI::EryD	This work.
*pGLD_D17*LE	Based on pET-22b(+)-GFP-LacO::DBS(1–200)-LacI::EryD	This work.
pErySensor	Core component in SMB	This work.
Primers		
pGZF	ttctcccttacccatatgtatatctccttcttaaagttaaacaaaattatttctag	
p181108ZR	gaactgtacaaaataagatccggctgctaacaaag	
DNS_F	ttaatttcgcgggatcgtatcaaacgccttcagcaatcctg	
DNS_R	cttctcccttacccatggctgacacaggctttcataaacat	
GFP_F	agcctgtgtcagccatgggtaagggagaagaacttttcact	
GFP_R	tcgagatctttatttgtacagttcatccatgccatgt	
Zai_F	atggatgaactgtacaaataaagatctcgatcctctacgccg	
Zai_R	aaggcgtttgatacgatcccgcgaaattaatacgactcac	
KE_F	ggtggtggtggccatatgtatatctccttc	
KE_R	tacatatggccaccaccaccaccaccactgagat	
KDG_K16F	atccggatgtttatgatgggtaagggagaagaacttttcact	
KDG_K16R	ttctcccttacccatcataaacatccggatttcctcccg	
KDG_rbsF	tatgaaagcctgaaggagtgtcagccatgggtaagggagaaga	
KDG_rbsR	ccatggctgacactccttcaggctttcataaacatccggatt	
pEryD_F	ttcagggtggtgaatatggcagatgcagacgattc	
pEryD_R	attaattgcgttgcgctcattttccattcggctggccgataaggg	
pDBS_F	tctccttcttaaagttaaacaaaattatttctagaggggctgacacaggctttcataaacatc	
p1-200inDBS_R	acgactcactataggcctttttagacgtagggtttt	
DBSU96_F	cgcatgttggagcctatagtgagtcgtattaatttcgc	
DBSU96_R	aatacgactcactataggctccaacatgcgccatcg	
DBSD17_F	aattatttctagaggataaacatccggatttcctcccg	
DBSD17_R	aatccggatgtttatcctctagaaataattttgtttaactttaagaaggagat	

at 6000 rpm for 1 min, and only 80 μl was kept for the cells to be fully suspended. Then the suspension was spread on the LB plate containing 100 μg/ml ampicillin. After cultured at 37 °C for 10 h, single colonies were selected for polymerase chain reaction (PCR) and sequencing verification (Nagamani et al., 2019).

2.4. Detection of fluorescence and erythritol

A ring of SMB strains solution was taken from a glycerol tube stored in refrigerator at -80 °C and inoculated in an aseptic culture tube containing 1 ml LB medium. After 9 h of incubation, 10 μl culture with OD_{600} of about 5 was inoculated in each unit of the 96-well plates with transparent bottom and opaque surroundings (Costa?R?*R*, REF 3603, Corning Incorporated). Then 180 μl of erythritol fermentation supernatant and 10 μl AMP-IPTG solution (Ampicillin 2 mg/ml, Isopropyl β-D-Thiogalactoside 10 mM) were added into each well. Subsequently, cultured at 37 °C, 700 rpm for 180 min in the orifice plate shaker, the whole plate was put into Cell Imaging Multi-Mode Reader (Cytation 5, Cell Imaging Reader from, BioTek, USA) for fluorescence intensity (FI) and OD_{600} detection. For parameters, it was vibrating 10 s to ensure uniformity and the gain value was set to 60%. The RFI is calculated as follows: RFI = FI/OD_{600}. There was a positive correlation between RFI value and erythritol concentration.

Accurate determination of erythritol and glucose in supernatant of fermentation broth was carried out by HPLC (1260 Infinity, Agilent, USA). Mobile phase: dilute sulfuric acid (5 mM); Column: Aminex?R?*R*HPX-87H Ion Exclusion Column; Column temperature: 40 °C; Flow rate: 0.6 ml/min; Detector: 1260 RID.

2.5. UV and ARTP mutagenesis

Mutant strains were obtained by combing mutagenesis of UV and ARTP (Guo et al., 2019), and then high-yield strains were screened by HTS established in this paper. A ring of *Yarrowia lipolytica* BBE-18 (CCTCC M 2019163, China Center for Type Culture Collection) strain was taken from a glycerol stock stored in refrigerator at -80 °C and inoculated in an aseptic culture tube containing 1 ml YPD medium. After incubation at 35 °C for 28 h, 400 μl of strains were added into 10 ml fresh YPD medium, and then incubated for 20 h. Subsequently, 4 ml strains were taken and centrifuged at 5000 rpm and the supernatant was discarded. The cell pellets were washed with physiological saline solution for two times, and then resuspended with 4 ml physiological saline solution and diluted to 40 ml in a 50 ml centrifuge tube as the initial strains solution for UV mutagenesis. The UV lamp power was 20 W and the irradiation distance is 30 cm. The mutagenesis is carried out under red light to avoid photorepair of the cells.

The preparation of the initial strains solution for ARTP mutagenesis is the same as for UV mutagenesis. The filling volume of each carrier is 10 μl. The ARTP irradiation power was 100 W, and the helium flow rate was 10 standard liter per minute (SLM) (Jin et al., 2018).

2.6. HTS of erythritol-producing strains of Yarrowia lipolytica

The mutant library of *Yarrowia lipolytica* BBE-18 was obtained by combined mutagenesis of UV and ARTP, and then erythritol-producing capacities of the oleaginous yeasts were sorted by the SMB system constructed in this work, and high-yield strains were selected. The specific HTS process is as follows:

The mutant strains obtained by combing mutagenesis were enriched and cultured to OD_{600} of 2 under dark conditions. Then the culture was diluted to 10^{-5}, and 100 μl of diluted strains were evenly spread on each plate. Then the strains were cultured in a constant temperature incubator at 35 °C for 40 h, 80–120 colonies were grown on each plate with a diameter of 1–2 mm.

Deep-well plates with each well of 2 ml were used and the fermentation medium HG was aliquoted into them by a liquid transfer workstation (Freedom EVO 200, TECAN, Switzerland). Then they were moved to the high throughput automatic microbial colony pick-up workstation (QPix420, Molecular Devices, USA) together with the plates full of colonies, and the colonies were quickly picked up and inoculated into the deep-well plates (Specific operation refers to the instructions of the equipment manufacturer). After inoculation, the deep-well plates were sealed with breathing freely cover and incubated at 35 °C for 10 days in orifice plate shakers. Then, the deep-well plates were centrifugated for 10 min at 4500 rpm. The supernatant was taken and used for fluorescence detection by the method described in 2.4. Then according to the RFI, high-yield strains were selected for further verification.

2.7. Production of erythritol by bench-top bioreactor

Small-scale fermentation experiments were carried out in 250 ml flasks with baffles at 35 °C and the speed is 220 rpm. The optimum strain *yliUA8* was further identified in a 3-liter fermenter (T&J Bioengineering Co. LTD, Shanghai, China). The aeration rate was 1.5 SLM and the rotational speed was 800 rpm. The HG fermentation medium was used for the production of erythritol with no control of pH during fermentation.

3. Results

3.1. Characterization of EryD as a novel erythritol sensor

EryD form *Brucella abortus* has been characterized as an activating type transcriptional factor and its activity is dependent on the effector molecule erythritol (Sangari et al., 2000). Previous studies on the function of EryD lacked mechanistic perspectives, leading to fragmented and ambiguous conclusions. In order to understand the mechanism, first we used the homology modeling tool SWISS-MODEL (https://swissmodel.expasy.org) to simulate the three-level structure of EryD and found that EryD had a high homology region with the L-sorbose-responsive transcriptional factor SorC (Sanctis et al., 2009). The homology model shows that EryD undergoes tetramerization and each of the unit contains a helix-turn-helix DNA binding domain (DBD) at the N-terminus of EryD. The binding domain of effector molecule (which is erythritol for this study) is localized in the C-terminus of the protein (Sanctis et al., 2009). The four subunits of this tetramer are labeled A, B, C, D, respectively. When erythritol presents, the tetramer falls apart into AD and BC dimers. Then, the AD dimer is detached from the DNA binding site, and the transcriptional initiation site is exposed to RNA polymerase for transcribing the downstream gene (Fig. 3) (Sanctis et al., 2009).

ITC assay has been reported as the most reliable and sensitive technique to determine binding constant and thermodynamic parameters for protein and nucleic acid interactions (Callies and Daranas, 2016). To experimentally validate the function of EryD, we performed ITC assay to quantify the binding process. Purified EryD protein (Fig. S1) was incubated with synthetic oligoes containing the DNA-binding sites for EryD in the presence or absence of erythritol. The isothermal titration curve between EryD and DBS at 25 °C is presented at Fig. 4a, while Fig. 4b represents a plot of the heat flow per injection of EryD

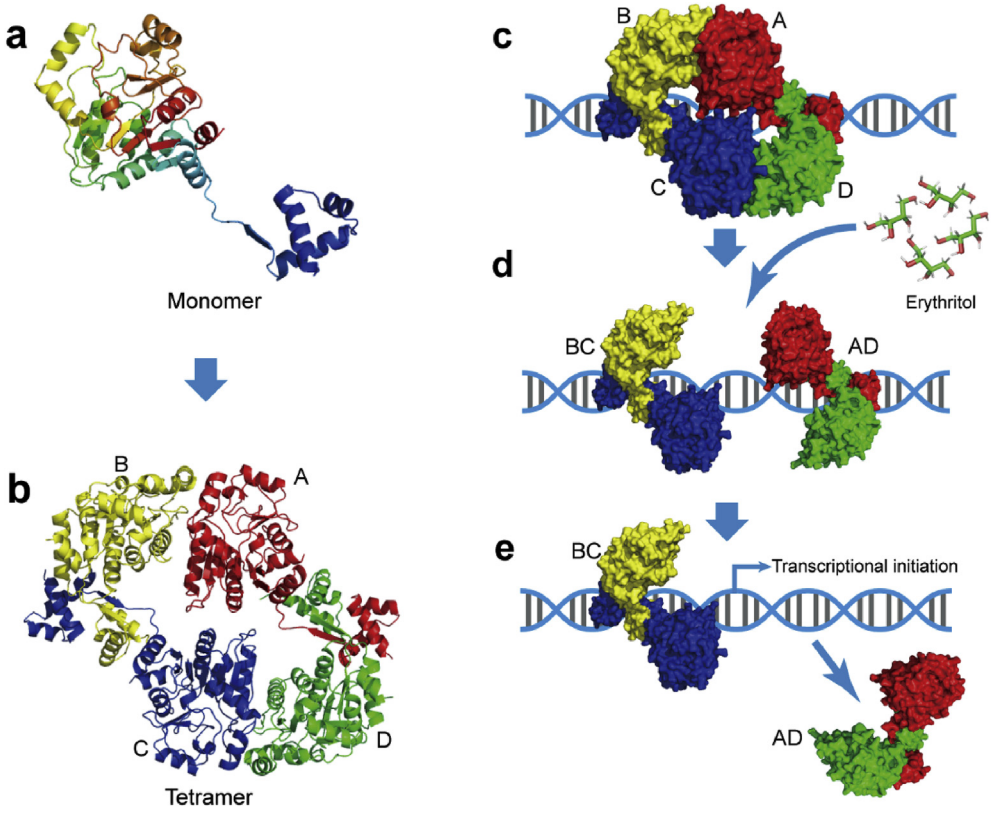

Fig. 3. Homology modeling reveals the transcriptional regulation mechanism of EryD. a. Monomeric structure of EryD; b. Tetramer structure of EryD; c. The EryD tetramer binds to DNA and forms a roadblock to prevent transcription; d. In the presence of erythritol, the tetramer falls apart into two dimers; e. The AD dimer is detached from DNA-binding site and the transcription initiation site is exposed for gene transcription.

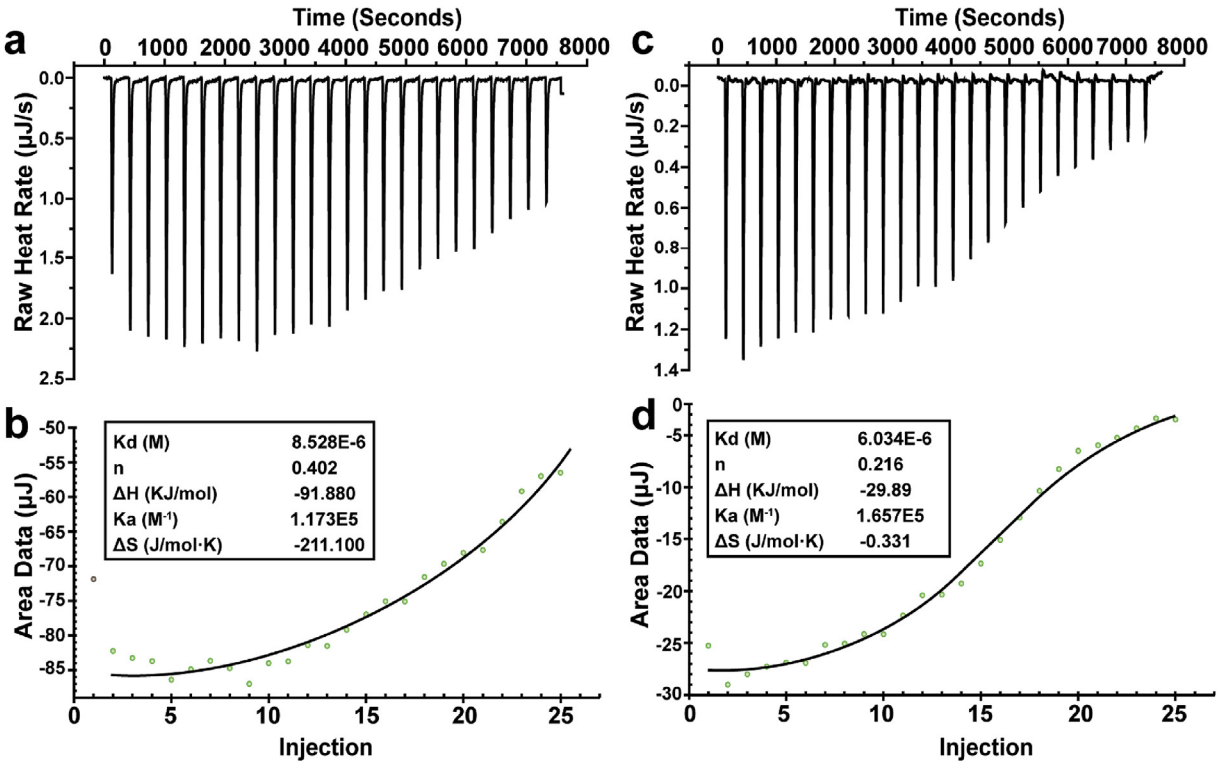

Fig. 4. Probing the binding affinity of EryD with putative operator and effector by ITC. (a) EryD to DBS: Raw heat rate changes with titration time. (b) EryD to DBS: Simulated curve of heat change with titration numbers and relevant parameters. (c) Erythritol to EryD: Raw heat rate changes with titration time. (d) Erythritol to EryD: Simulated curve of heat change with titration numbers and relevant parameters.

versus the molar ratio of protein and DBS. The data was reported after subtraction of the background titration. We calculated and summarized the parameters determined by ITC (Fig. 4b). The values of equilibrium binding constant Ka and entropy change ΔS indicate moderate binding affinity between EryD and the operator sequence.

When erythritol appears, EryD will dissociate from the operator. Erythritol solution was used to titrate EryD and the values of ΔH and ΔS demonstrated strong negative values, indicating that the binding of EryD with erythritol is an exothermic reaction, possibly due to hydrogen bonding and hydrophobic interaction (Debowski et al., 2016). The equilibrium binding constant Ka and dissociation constant Kd confirmed the binding affinity of EryD with erythritol (Fig. 4c and d).

Thermodynamic laws for determining the interaction between biological macromolecules and small molecules have been well summarized by Ross et al. (Ross and Subramanian, 1981). They found that when $\Delta H \geq 0$ and $\Delta S > 0$, the major interaction is hydrophobic force; when $\Delta H < 0$ and $\Delta S > 0$, the major interaction is the electrostatic force; when $\Delta H < 0$ and $\Delta S < 0$, the major interaction is Van Der Waals or the hydrogen bond force. On the basis of the ITC data (Fig. 4), the binding of EryD with DBS sequence is mainly dominated by Van Der Waals or hydrogen bonding force. However, the interaction between EryD and erythritol is relatively weak by Van Der Waals force and hydrogen bonding force, it is possible that electrostatic force plays a major role considering the highly charged amino acid residue of the C-terminal domain of EryD. The electrostatic interaction between erythritol and EryD is relatively weak and it is vulnerable to other solutes, so it is important for us to optimize the fermentation substrates especially glucose in practical application, which will be described in part 3.3.

3.2. The construction of SMB for the screening of erythritol-producing strains

We next sought to construct a hybrid promoter-regulator system by harnessing the versatility of T7 promoter (Xu et al., 2012, 2014). To explore the optimal genetic configuration of EryD (Table 1), we first constructed a hybrid T7-EryD system by inserting a 951 bp region that coding EryD downstream of T7 promoter (Wu et al., 2018). We did not know the specific length of the Ery promoter, in order to ensure its complete function, 742 bp upstream of EryA containing the Ery promoter-operator was taken as the hypothetical Ery promoter (Fig. S2) (Zhang et al., 2016). The green fluorescent protein gene *eGFP* was placed downstream of the promoter as a reporter. Upon transformed into *E. coli* BL21(DE3) (Fig. S2a), we didn't observe any fluorescence signals. We speculate there are two possible reasons: one is the leakage expression of EryD by T7 promoter, which strongly represses expression of the Ery promoter-operator and the downstream eGFP reporter; the other is that the Ery Operon promoter failed to start successfully in *E. coli* BL21(DE3).

To troubleshoot and test whether this transcriptional repression is caused by EryD leakage expression, we knocked out *EryD* from the plasmid and found that there was still no detectable fluorescent protein expression (Fig. S2b). So we can rule out the leaky expression. In order to understand why Ery Operon didn't function in *E. coli* BL21(DE3), we speculate that the large distance between ribosome binding sites (RBS) and the start codon precludes efficient translation initiation, or that the RBS cannot function properly. To test this hypothesis, we checked the DNA sequence upstream of the start codon of *eGFP* and found a GA-rich possible RBS sequence “GAGGA”, which is about 32 bp upstream of the initial codon of *eGFP*. We next knocked out 16 bp upstream of the initial codon of the *eGFP*, shortening the distance between the start codon of *eGFP* and the presumed RBS. Unexpectedly, we still couldn't detect any fluorescence signals (Fig. S2c). Then, the RBS sequence “AAGGAG” (which originates from pET-22b(+) plasmid) was inserted upstream of the initial codon of the *eGFP*. There was 8 bp distance from the translation initiation site “ATG”, still, no fluorescent signals could be detected (Fig. S2d). Finally, we concluded that Ery promoter-operator sequence could not drive gene transcription in *E. coli* BL21(DE3), this

non-portability maybe indicates the distinct transcription mechanism between *E. coli* and *Brucella abortus*.

On the basis of above experiments, we planned to remove the lactose repressor binding site LacO and installed an EryD binding sequence and *eGFP* directly proceeding with the T7 promoter. Generally, the repressor-binding DNA sequence lies between RBS and promoter sequence, and the sequence is not too long. To simplify this, we selected 200 bp upstream of EryA start codon as a possible DBS sequence to replace LacO. Then, *EryD* was placed under a constitutive promoter. After successful construction and transformation of *E. coli* BL21(DE3), we still couldn't detect eGFP with the presence of IPTG and erythritol. We continued to shorten the DBS sequence from the 5′ end. When this operator (EryD-binding region) was shortened to 104 bp, we detected strong eGFP expression. Upon induction with erythritol, we detected much brighter signal than that of non-erythritol induction (Fig. 5), indicating the functionality of the EryD sensor.

3.3. Characterization of the sensor-regulator system

In order to test the effectiveness of the sensor-regulator system, we quantified the fluorescence signals with different concentrations of erythritol. IPTG was added at the same time to reach the induction concentration mentioned above. The fluorescence signals were detected after incubation at 37 °C for 6 h. We found that the sensor-operator didn't output obvious fluorescence signals with 1–100 mM of erythritol. Between 250 and 500 mM, we observed that the fluorescence output was positively correlated with the concentration of erythritol. However, further increasing erythritol to 1000 mM didn't yield improved fluorescence as compared to 500 mM erythritol. This suggest that the input response range of the sensor-regulator to erythritol was estimated at 250–500 mM (Fig. 6a).

High level of glucose is used as fermentation substrate in the commercial production of erythritol. If the SMB system is going to be used as a high throughput detection tool, high level of glucose may impact the dose-response curve of the sensor system negatively. In the experiments of erythritol fermentation with deep-well plates, the optimal concentration of glucose in fermentation medium is 150 g/L (Fig. 8b), and the residual glucose concentration after fermentation is normally maintained at about 100 g/L (Fig. S3). Therefore, we added 100 g/L of glucose to the medium for SMB strains to simulate the actual fermentation scenario. We next determined the dose-response of the constructed sensor with 5 mM, 10 mM, 50 mM, 100 mM, 250 mM and 500 mM of erythritol. Interestingly, the sensor-regulator became more sensitive to erythritol, with an input erythritol concentration ranging from 5 to 250 mM (Fig. 6b). Then, we tested erythritol of different gradients (1 mM, 5 mM, 10 mM, 50 mM, 100 mM, 200 mM, 250 mM, 300 mM, 400 mM and 500 mM) under various concentrations of glucose with the SMB system and found that when the glucose concentration was 50–140 g/L, the response interval was basically the same (Fig. 7). With the addition of glucose, the sensitivity of the microbial sensing system is improved. The specific mechanism is not yet clear, and this may be the characteristic of EryD from *Brucella abortus* (Sangari et al., 2000).

3.4. Optimizing high throughput fermentation with deep-well plates

High throughput fermentation is the first step to achieve high throughput screening (Nemeth, 2017). Therefore, we explored the possibility of using deep-well plates to develop a high throughput fermentation process. *Yarrowia lipolytica* is an aerobic yeast which requires higher dissolved oxygen to produce erythritol. The deep-well plates were sealed with film and stainless steel cover with breathable paper, respectively. At the same time, we varied the glucose from 300 g/L, 200 g/L, 150 g/L, 100 g/L to 50 g/L. After 10 days of fermentation, yeast growth was confirmed by detecting OD_{600}. When stainless steel cover was used and compared with using film, the value of OD_{600} remained more similar to shaking flask fermentation (Fig. 8a).

Erythritol titer from the deep-well plate was determined by HPLC.

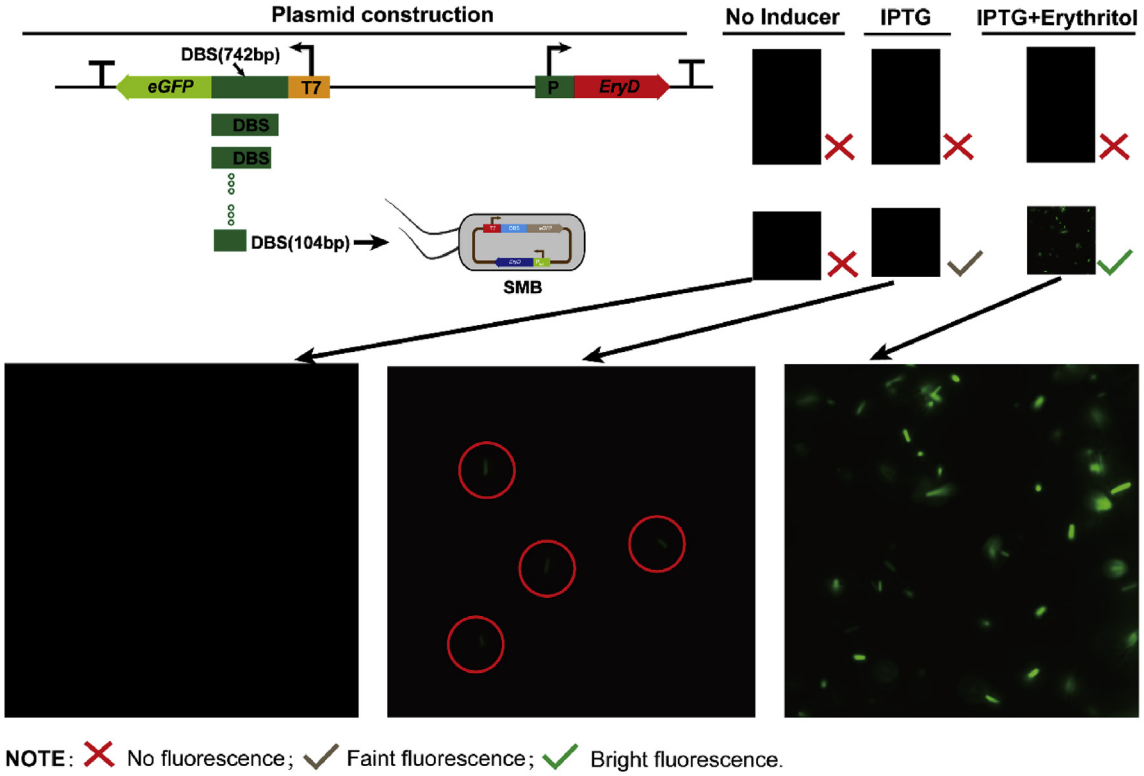

Fig. 5. Optimal sensor construct by using truncated EryD-binding sequeces. With the final SMB, eGFP expressed successfully with the inducement of IPTG and Erythritol.

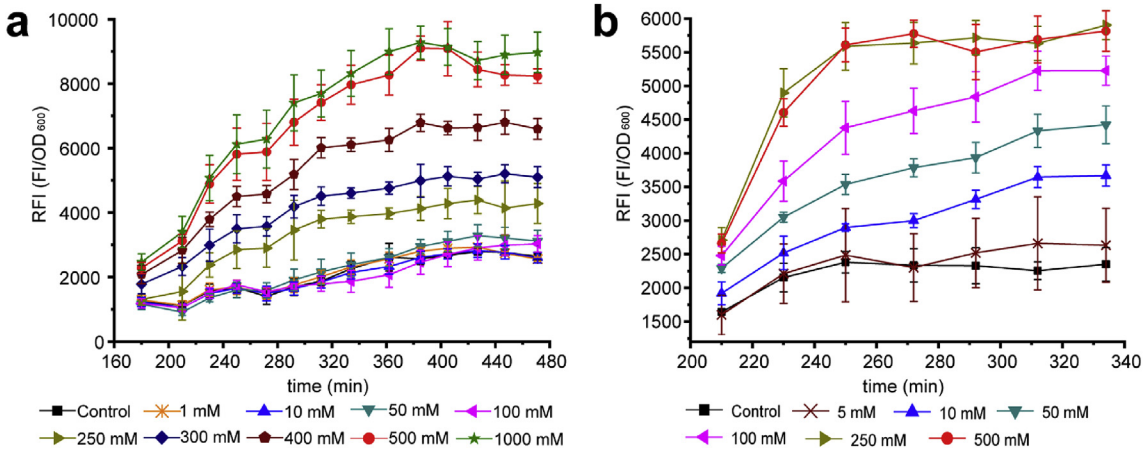

Fig. 6. Dose-responses of the SMB to erythritol. a. Fluorescence signals induced by pure erythritol ranging from 1 to 1000 mM; b. Fluorescence signals induced by varying concentration of erythritol mixed with 100 g/L glucose.

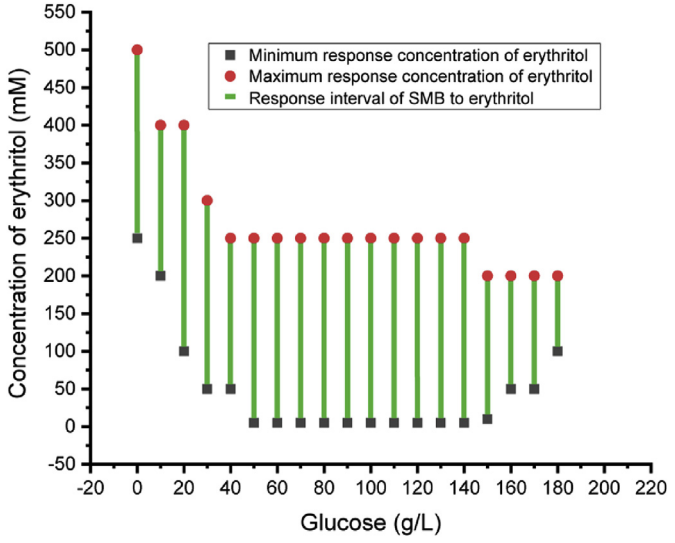

Fig. 7. Response range of SMB to erythritol under different concentrations of glucose.

We found that the erythritol level was within the detection range of our SMB system when the initial glucose was 100–300 g/L (Fig. 8b). When the initial glucose concentration was 150 g/L, the yield of erythritol was the highest which was in the conducive to SMB response. Using the fermentation supernatant containing different levels of erythritol (Fig. 8b), we cultured the *E. coli* strains harboring the EryD sensor-regulator system. We found that the sensor strain (*E. coli* harboring the EryD sensor-regulator system) could grow normally with the fermentation supernatant from initial glucose of 100 and 150 g/L, and the growth presented a typical S-shaped sigmoidal curve (Fig. 8c). Through the above study, we used the initial glucose concentration of 150 g/L for high throughput fermentation with deep-well plates. Next, we added different concentrations of erythritol to the supernatant from deep-well plate fermentation under this condition to simulate the different erythritol-producing capacities of the mutant library, and then detected it with SMB system and HPLC, respectively. From the test results, it can be found that the SMB system and HPLC test results showed a linear correlation (Fig. 8d). These findings confirmed that the sensor strain constructed in this work can be used reliably for high throughput screening of erythritol overproducers.

3.5. Screening of a mutant library to improve erythritol production

UV and ARTP mutagenesis are commonly used for microbial breeding (Ottenheim et al., 2018; Yamada et al., 2017). Because of the ease of operation and non-toxicity, both UV and ARTP have been widely adopted by microbial breeding researchers (Ameri et al., 2019; Ottenheim et al., 2018). With appropriate exposure time of UV and ARTP, we first determined the survival rate of *Yarrowia lipolytica* by evaluating a gradient irradiation time. In UV mutagenesis, the selected irradiation time was 60 s, and the fatality rate was 87.4%. The optimal exposure time for ARTP was 45 s and the fatality rate was 86.6% (Fig. 10a). By combining UV mutagenesis with ARTP mutagenesis, 12 plates coated with *Yarrowia lipolytica* mutant strains were obtained. Then, each single colony on the plates was individually transferred to deep-well plates with 900 μl/well HG fermentation medium by using high-throughput microbial inoculation system. In this work, we built a library containing 1152 mutant strains with UV and ARTP combinatorial mutagenesis. Each colony of the mutant library was inoculated and cultured in deep-well plates at 35 °C and 220 rpm for 10 days. High throughput screening of erythritol-producing strains was carried out using the SMB sensor-regulator system constructed in this paper, which was based on the transcriptional factor EryD. Among the mutant library, the erythritol-producing capacities of 186 strains were higher than that of the initial strain (Fig. 9).

The fermentation performances of the 1152 strains were sorted for erythritol production. The specific implementation steps were automated and can be referred to part 2.4. After sorting, fifteen strains with better yield were selected for fermentation verification in 250 ml flasks with 50 ml HG media in each. After 76 h of cultivation, all the glucose was consumed. Strain *yliUA8* produced 103 g/L erythritol, it was 2.4-fold compared to the initial strain (*Yarrowia lipolytica* BBE-18 produced 43 g/L erythritol). In order to ensure the accuracy, three parallel experiments were conducted (Fig. 10b). Among the fifteen strains of the erythritol-producing strains screened, the by-products of *yliUA6*, *yliUA8*, *yliUA12* and *yliUA14* were significantly lower than that of the original strain *Yarrowia lipolytica* BBE-18, which favors industrial application due to easy downstream purification (Fig. 10c).

To further verify the fermentation performance of *yliUA8*, this strain was cultivated in a 3-liter fermenter (Fig. 10d). During the fermentation process, the cell density (OD_{600}) increased rapidly from 0.08 to 107 in 20 h, and the pH decreased rapidly from 6.17 to 2.99. At growth phase of logarithmic mid-term, dissolved oxygen (DO) dropped to lowest 40.6%, and then the DO rebounded rapidly. After entering the stable period, the OD_{600} maintained at a stable value. Before the exponential growth period, erythritol productivity was very low. After entering the stable growth period, the titer of erythritol was linearly increasing with

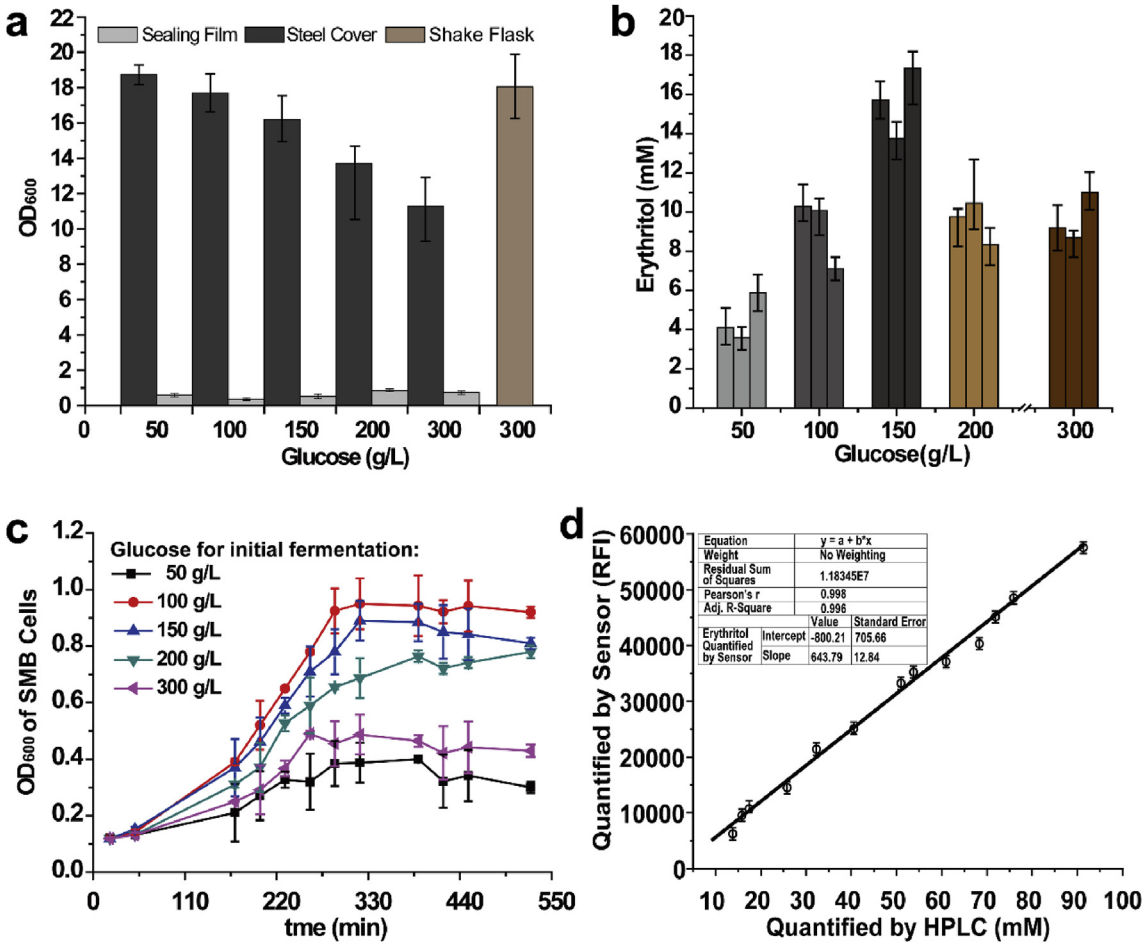

Fig. 8. High throughput fermentation optimization in deep-well plates and the correlation between HPLC and SMB detection of erythritol. a. Comparison of OD_{600} of different initial glucose titer that fermented in deep-well plates with shaking flasks. b. Erythritol fermented with gradients of glucose in deep-well plates and detected by HPLC. Each of three columns represents three different batches under each glucose concentration, and every batch has three parallels. c. Growth curve of the SMB cells with erythritol fermentation supernatant which is fermented with gradients of glucose as substrate. d. The correlation between SMB and HPLC was determined by detecting the supernatants of fermentation with different erythritol concentrations.

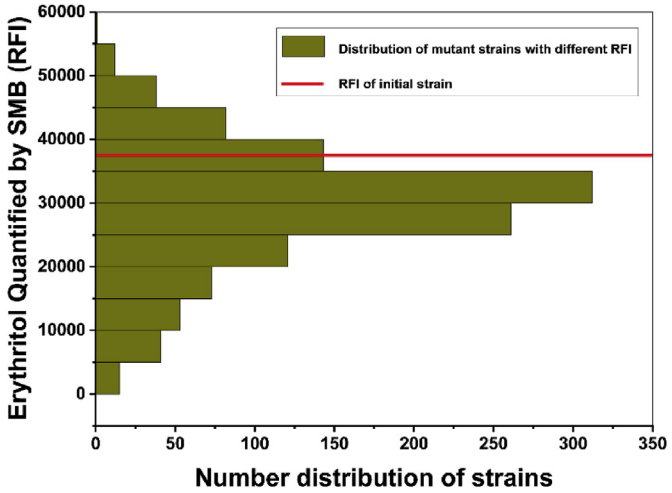

Fig. 9. Distribution of erythritol-producing capacities of the mutant library sorted by SMB system.

the fermentation time. Then, the value of OD_{600} decreased gradually, indicating the occurrence of strain death. After 95 h of fermentation, the value of OD_{600} decreased to 57, and the maximum erythritol production reached 148 g/L. The initial glucose concentration of the 3-liter fermenter is 165 g/L. During the fermentation process, 500 ml glucose solution (500 g/L) was intermittently supplemented to the bioreactor to maintain enough substrate. Glucose supplementation was carried out in the stable growth period, because a large amount of glucose had been consumed during the exponential growth period.

4. Discussion

Transcriptional factor based biosensor is a powerful tool for high throughput strain screening (Johnson et al., 2017; Wan et al., 2019; Xu, 2018; Yu et al., 2019). Nevertheless, there are few reports on developing biosensors to detect polyols. Among many biosensors, BmoR can respond to alkane alcohols, including n-butanol, isobutanol, 3-methyl-1-butanol, n-pentanol, n-hexanol, n-heptanol and other alcohols et al. It has been successfully used for screening high butanol-producing strains, however, no attempt has been made to apply on sugar polyols (Yu et al., 2019). Park et al. have identified four upstream activation sequences (UAS), which are involved in transcription induction by erythritol, but none of the identified UAS has been applied for high throughput screening of erythritol overproducers (Park et al., 2019). In addition, Savergave et al. screened erythritol-producing strains by reduced discoloration of TTC. However, the correlation between erythritol production and reductase activity is ambiguous and less specific, possibly due to too many reductases inside the cells (Savergave et al., 2011).

To test whether the SMB system could respond to other sugar

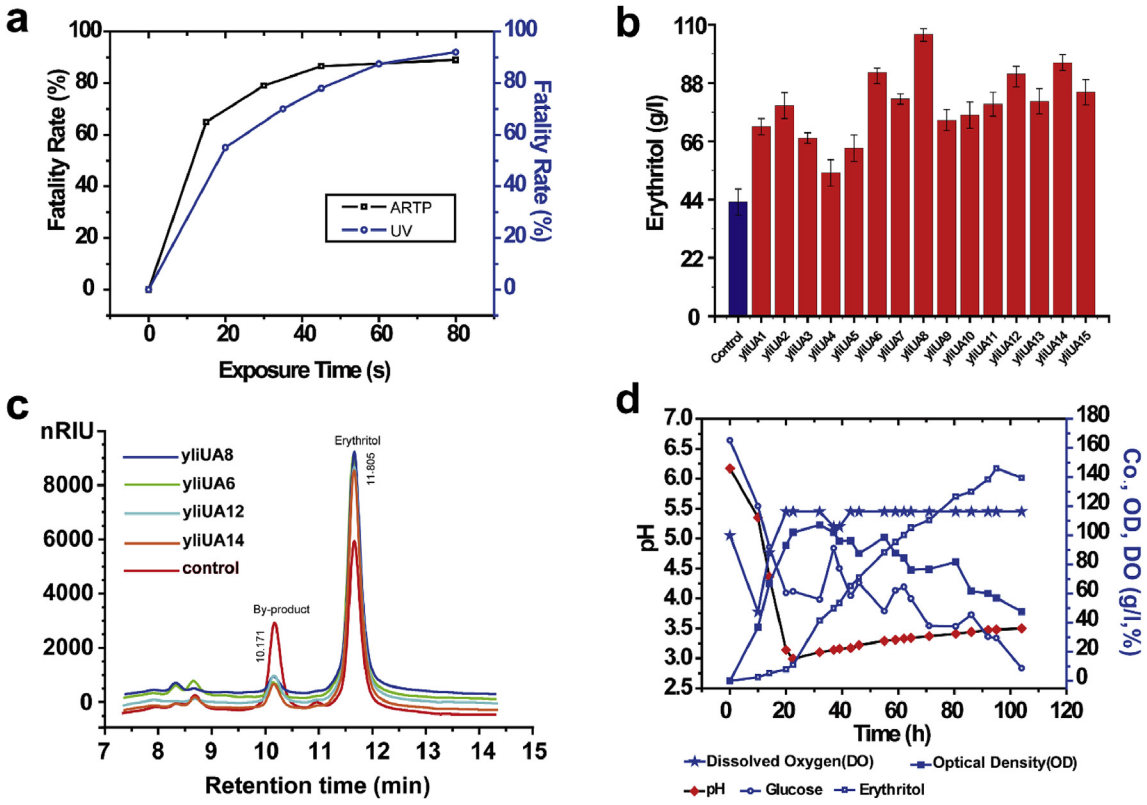

Fig. 10. Screening of high-yield erythritol-producing strains with the sensor-regulator system. a. The relationships between exposure time and lethality of *Yarrowia lipolytica* respectively in UV and ARTP mutagenesis. b. Contrast of erythritol production between the *Yarrowia lipolytica* BBE-18 (control) and the fifteen *Yarrowia lipolytica* strains screened by SMB system in 250 ml flasks. c. Comparison of by-products between the original strain and the screened optimum four strains. d. Erythritol Production by the optimal strain *yliUA8* in a 3-liter fermenter.

polyols, we used sorbitol, maltitol and lactitol to probe the dose response. Different gradients of each polyol (10 mM, 50 mM, 100 mM, 250 mM, 500 mM) were used as input concentration range. We observed that the sensor-regulator system could respond to all these polyols. Among these polyols, the SMB system has a good response to sorbitol above 50 mM. It is not sensitive to maltitol and lactitol when they are below 100 mM, but when the concentration is above 250 mM, they are responded with strong fluorescence signals by the SMB system. This makes it possible to extend the sensor-regulator system for detection and high throughput screening of other polyol-producing strains. It is noteworthy that the response of the sensor-regulator system to these polyols decreases with time (Fig. S4).

In the SMB system we constructed, the repression of EryD on T7 promoter is not complete. In the absence of erythritol, there will be slight leakage expression when just induced by IPTG (Fig. 5). Although this does not affect our application in the high throughput screening of erythritol overproducing strains, it provides us with further research spaces.

5. Conclusion

We constructed a sensor-regulator system based on the erythritol-responsive transcriptional factor EryD, and successfully applied it as a high throughput screening method for the characterization of erythritol overproducers. With the sensor-regulator system, we rapidly characterized a strain library containing 1152 mutants derived from combined UV and ARTP mutagenesis. We obtained a high erythritol producers *yliUA8* with few by-products, this strain produced 148 g/L erythritol in a 3-liter fermenter. Moving forward,we tested the specificity of the sensor-regulator system toward other sugar polyols including sorbitol, lactitol and maltitol. The reported framework enables us to rapidly improve strain performance and engineer efficient microbial cell factories for industrial applications.

Acknowledgements

The authors would like to acknowledge financial support of the National Key Research and Development Program of China (2017YFB0308401), the 111 project (111-2-06), the grant from Pioneer Innovative Research Team of Dezhou, the National First-class Discipline Program of Light Industry Technology and Engineering (LITE2018-08), the National Key Research and Development Program of China (2019YFC1605800) and the Open Project of Key Laboratory of Industrial Biotechnology, Ministry of Education, Jiangnan University (KLIB-KF201706).

Appendix A. Supplementary data

Supplementary data to this article can be found online at https://doi.org/10.1016/j.ymben.2020.03.006.

References

Albers, E., Larsson, C., 2009. A comparison of stress tolerance in YPD and industrial lignocellulose-based medium among industrial and laboratory yeast strains. J. Ind. Microbiol. Biotechnol. 36, 1085–1091.

Ameri, A., Shakibaie, M., Soleimani-Kermani, M., Faramarzi, M.A., Forootanfar, H., 2019. Overproduction of thermoalkalophilic lipase secreted by *Bacillus atrophaeus* FSHM2 using UV-induced mutagenesis and statistical optimization of medium components. Prep. Biochem. Biotechnol. 49, 184–191.

Barbier, T., Zuniga-Ripa, A., Moussa, S., Plovier, H., Sternon, J.F., Lazaro-Anton, L., Conde-Alvarez, R., De Bolle, X., Iriarte, M., Moriyon, I., Letesson, J.J., 2018. *Brucella* central carbon metabolism: an update. Crit. Rev. Microbiol. 44, 182–211.

Bolognese, F., Scanferla, C., Caruso, E., Orlandi, V.T., 2019. Bacterial melanin production by heterologous expression of 4 hydroxyphenylpyruvate dioxygenase from

Pseudomonas aeruginosa. Int. J. Biol. Macromol. 133, 1072–1080.
Callies, O., Daranas, A.H., 2016. Application of isothermal titration calorimetry as a tool to study natural product interactions. Nat. Prod. Rep. 33, 881–904.
Carly, F., Fickers, P., 2018. Erythritol production by yeasts: a snapshot of current knowledge. Yeast 35, 455–463.
Carly, F., Vandermies, M., Telek, S., Steels, S., Thomas, S., Nicaud, J.M., Fickers, P., 2017. Enhancing erythritol productivity in *Yarrowia lipolytica* using metabolic engineering. Metab. Eng. 42, 19–24.
Dai, L., Tai, C., Shen, Y.L., Guo, Y.L., Tao, F., 2019. Biosynthesis of 1,4-butanediol from erythritol using whole-cell catalysis. Biocatal. Biotransform. 37, 92–96.
Debowski, D., Wyrzykowski, D., Lubos, M., Rolka, K., 2016. Interactions between trypsin and its peptidic inhibitors studied by isothermal titration calorimetry (ITC). J. Therm. Anal. Calorim. 123, 807–812.
Gibson, D.G., Glass, J.I., Lartigue, C., Noskov, V.N., Chuang, R.Y., Algire, M.A., Benders, G.A., Montague, M.G., Ma, L., Moodie, M.M., Merryman, C., Vashee, S., Krishnakumar, R., Assad-Garcia, N., Andrews-Pfannkoch, C., Denisova, E.A., Young, L., Qi, Z.Q., Segall-Shapiro, T.H., Calvey, C.H., Parmar, P.P., Hutchison, C.A., Smith, H.O., Venter, J.C., 2010. Creation of a bacterial cell controlled by a chemically synthesized genome. Science 329, 52–56.
Gibson, D.G., Young, L., Chuang, R.Y., Venter, J.C., Hutchison, C.A., Smith, H.O., 2009. Enzymatic assembly of DNA molecules up to several hundred kilobases. Nat. Methods 6 343-U41.
Guo, M.R., Cheng, S.B., Chen, G.G., Chen, J.L., 2019. Improvement of lipid production in oleaginous yeast *Rhodosporidium toruloides* by ultraviolet mutagenesis. Eng. Life Sci. 19, 548–556.
Jin, J., Wang, Y., Yao, M.D., Gu, X.L., Li, B., Liu, H., Ding, M.Z., Xiao, W.H., Yuan, Y.J., 2018. Astaxanthin overproduction in yeast by strain engineering and new gene target uncovering. Biotechnol. Biofuels 11, 15.
Jira, J., Rezek, B., Kriha, V., Artemenko, A., Matolinova, I., Skakalova, V., Stenclova, P., Kromka, A., 2018. Inhibition of *E. coli* growth by nanodiamond and graphene oxide enhanced by Luria-Bertani medium. Nanomaterials 8, 13.
Johnson, A.O., Gonzalez-Villanueva, M., Wong, L., Steinbüchel, A., Tee, K.L., Xu, P., Wong, T.S., 2017. Design and application of genetically-encoded malonyl-CoA biosensors for metabolic engineering of microbial cell factories. Metab. Eng. 44, 253–264.
Mahmood, M.S., Rasul, F., Saleem, M., Afroz, A., Malik, M.F., Ashraf, N.M., Rashid, U., Naz, S., Zeeshan, N., 2019. Characterization of recombinant endo-1,4-beta-xylanase of *Bacillus halodurans* C-125 and rational identification of hot spot amino acid residues responsible for enhancing thermostability by an in-silico approach. Mol. Biol. Rep. 46, 3651–3662.
Nagamani, G., Alex, S., Soni, K.B., Anith, K.N., Viji, M.M., Kiran, A.G., 2019. A novel approach for increasing transformation efficiency in *E. coli* DH5 cells using silver nanoparticles. 3 Biotech 9, 7.
Nemeth, A., 2017. Examination of innovative high-throughput fermentations. Hungar. J. Ind. Chem. 45, 19–21.
Ottenheim, C., Nawrath, M., Wu, J.C., 2018. Microbial mutagenesis by atmospheric and room-temperature plasma (ARTP): the latest development. Bioresour. Bioprocess. 5, 14.
Park, Y.K., Korpys, P., Kubiak, M., Celinska, E., Soudier, P., Trebulle, P., Larroude, M., Rossignol, T., Nicaud, J.M., 2019. Engineering the architecture of erythritol-inducible promoters for regulated and enhanced gene expression in *Yarrowia lipolytica*. FEMS Yeast Res. 19.
Raymundo, J.F., Oliveski, R.D., Rocha, L.A.O., Biserni, C., 2018. Numerical investigation on phase change materials (PCM): the melting process of erythritol in spheres under different thermal conditions. Int. J. Mech. Sci. 148, 20–30.
Ross, P.D., Subramanian, S., 1981. Thermodynamics of protein association reactions: forces contributing to stability. Biochemistry 20, 3096–3102.
Sanctis, D.d., McVey2, C.E., Enguita, F.J., Carrondo, M.A., McVey, C.E., Enguita, F.J., Carrondo, M.A., 2009. Crystal structure of the full-length sorbitol operon regulator SorC from *Klebsiella pneumoniae*: structural evidence for a novel transcriptional regulation mechanism. J. Mol. Biol. 387, 759–770.
Sangari, F.J., Aguero, J., Garcia-Lobo, J.M., 2000. The genes for erythritol catabolism are organized as an inducible operon in *Brucella abortus*. Microbiol. SGM 146, 487–495.
Savergave, L.S., Gadre, R.V., Vaidya, B.K., Narayanan, K., 2011. Strain improvement and statistical media optimization for enhanced erythritol production with minimal by-products from *Candida magnoliae* mutant R23. Biochem. Eng. J. 55, 92–100.
Silva, L.V.d., Coelho, M.A.Z., Amaral, P.F.F., Fickers, P., 2018. A novel osmotic pressure strategy to improve erythritol production by *Yarrowia lipolytica* from glycerol. Bioproc. Biosyst. Eng. 41, 1883–1886.
Tshibalonza, N.N., Gerardy, R., Alsafra, Z., Eppe, G., Monbaliu, J.C.M., 2018. A versatile biobased continuous flow strategy for the production of 3-butene-1,2-diol and vinyl ethylene carbonate from erythritol. Green Chem. 20, 5147–5157.
Wan, X., Marsafari, M., Xu, P., 2019. Engineering metabolite-responsive transcriptional factors to sense small molecules in eukaryotes: current state and perspectives. Microb. Cell Factories 18, 61.
Wang, F., Zhan, X., Zheng, Z., Wu, J., Yuan, B., Cai, L., 2013. Mutation screening and identification of osmophilic yeast for erythritol production. Ind. Microbiol. 43, 59–63.
Wu, J., Fan, X.C., Liu, J., Luo, Q.L., Xu, J.S., Chen, X.L., 2018. Promoter engineering of cascade biocatalysis for alpha-ketoglutaric acid production by coexpressing L-glutamate oxidase and catalase. Appl. Microbiol. Biotechnol. 102, 4755–4764.
Xu, P., 2018. Production of chemicals using dynamic control of metabolic fluxes. Curr. Opin. Biotechnol. 53, 12–19.
Xu, P., Vansiri, A., Bhan, N., Koffas, M., 2012. ePathBrick: a synthetic biology platform for engineering metabolic pathways in *E-coli*. ACS Synth. Biol. 1, 256–266.
Xu, P., Wang, W., Li, L., Bhan, N., Zhang, F., Koffas, M.A.G., 2014. Design and kinetic analysis of a hybrid promoter-regulator system for malonyl-CoA sensing in *Escherichia coli*. ACS Chem. Biol. 9, 451–458.
Yamada, R., Yamauchi, A., Kashihara, T., Ogino, H., 2017. Evaluation of lipid production from xylose and glucose/xylose mixed sugar in various oleaginous yeasts and improvement of lipid production by UV mutagenesis. Biochem. Eng. J. 128, 76–82.
Yu, H., Chen, Z., Wang, N., Yu, S., Yan, Y., Huo, Y.-X., 2019. Engineering transcription factor BmoR for screening butanol overproducers. Metab. Eng. 56, 28–38.
Zhang, G.Q., Lin, Y.P., Qi, X.N., Wang, L.X., He, P., Wang, Q.H., Ma, Y.H., 2015. Genome shuffling of the nonconventional yeast *Pichia anomala* for improved sugar alcohol production. Microb. Cell Factories 14, 10.
Zhang, H., Dou, X.X., Li, Z.Q., Zhang, Y., Zhang, J., Guo, F., Wang, Y.Z., Wang, Z., Li, T.S., Gu, X.L., Chen, C.F., 2016. Expression and regulation of the Ery Operon of *Brucella melitensis* in human trophoblast cells. Exp. Ther. Med. 12, 2723–2728.
Zhang, J., Yin, S., Guo, F., Meng, R., Chen, C., Zhang, H., Li, Z., Fu, Q., Shi, H., Hu, S., Ni, W., Li, T., Zhang, K., 2014. A potent *Brucella abortus* 2308 Δ*ery* live vaccine allows for the differentiation between natural and vaccinated infection. J. Microbiol. 52, 681–688.
Zheng, S., Hou, J., Zhou, Y., Fang, H., Wang, T.T., Liu, F., Wang, F.S., Sheng, J.Z., 2018. One-pot two-strain system based on glucaric acid biosensor for rapid screening of myo-inositol oxygenase mutations and glucaric acid production in recombinant cells. Metab. Eng. 49, 212–219.